Insertion Devices in the First Year at Taiwan Photon Source

TPS is a new medium-energy highly brilliant synchrotron light facility. The commissioning of the storage ring was completed by December 2014. Electron emittance and emittance coupling were measured at 1.6 nmrad and 0.01 %, respectively. To utilize the small emittance and great quality of the electron beam to achieve a highly brilliant light source, a mini-gap in-vacuum undulator is used for hard X-ray photons. Polarization control in soft X-ray photon sources involves use of elliptically polarized undulators (EPU). To ensure a highly brilliant light source and stable operation of the storage ring demands a stringent field quality of undulators. Ten phase-I insertion devices (ID) were installed in April and commissioning began in September 2015. This report presents the undulator performance, the experience and the results of installation and commissioning of the TPS ID.

Introduction

Undulators are the main light sources to generate intense radiation at the TPS. In-vacuum undulators and EPU are used to provide hard and soft X-ray for Phase-I beamlines respectively. Table 1 summarizes the parameters of phase-I ID at the TPS. A double undulator configuration (I09, I23, I41) is installed in the 12-m straight section. As is well known, an increasing number of undulator periods is a direct approach to increase the brilliance of radiation from an undulator. For a long undulator, a small undulator gap is unsuitable because a short beam lifetime is expected. A long undulator can hence be divided into two or three segmented undulators, and accommodated in the minimum vertical betatron function of each section to maintain an acceptable beam lifetime. If constructive interference is preserved between two wave packets of undulator radiation, the brilliance of a double collinear undulator configuration might be enhanced relative to a single undulator.

To avoid accident caused by upstream synchrotron radiation heatload in a double-IU configuration, a vertical photon absorber is installed to protect magnet cover at an in-vacuum undulator downstream.[1] Installation and commissioning of a double-undulator configuration therefore requires great effort to ensure that the two undulator radiation cones overlap maximally, emitted onto the magnet cover.

Installation of insertion devices

Since April 2015, ten IDs (7 in-vacuum undulators and 3 EPU) have been installed in the TPS tunnel (Fig. 1). After their installation, alignment and leveling of all IDs were performed. Undulator leveling must be adjusted within ± 10 μm/m from a leveling condition recorded in the measurement laboratory and alignment to the storage ring position must be within ± 50 μm. As in-vacuum undulators share the vacuum with the storage ring, baking is necessary (Fig. 2). To achieve a tight time schedule, baking seven IU22 must be completed within eight weeks and two IU22 must be baked at the same time. The total duration of baking was 60 h, of which the first 10 h involved

Table 1: List of phase-I ID.

Port	Type	Period length (mm)	No. of periods	Gap (mm)	Effective field (T)
05	IU	22	140	7 5.6	0.79 (1.02*)
09	IU	22	140	7 5.5	0.74 (0.96*)
	IU	22	95	7	0.72
21	IU+Taper	22	140	7 5.5	0.75 (0.98*)
23	IU	22	140	7 5.5	0.73 (0.95*)
25	IU	22	140	7 5.5	0.75 (0.98*)
	IU	22	95	7	0.73
41	EPU	48	68	14	0.84/0.55
	EPU	48	68	14	0.84/0.55
45	EPU	46	82	13	0.79/0.52

* Mechanical minimum undulator gap.

Fig. 1: Gallery of installation of in-vacuum undulators in the storage ring.

Fig. 2: Gallery of IU22-3 m baked at TPS storage ring.

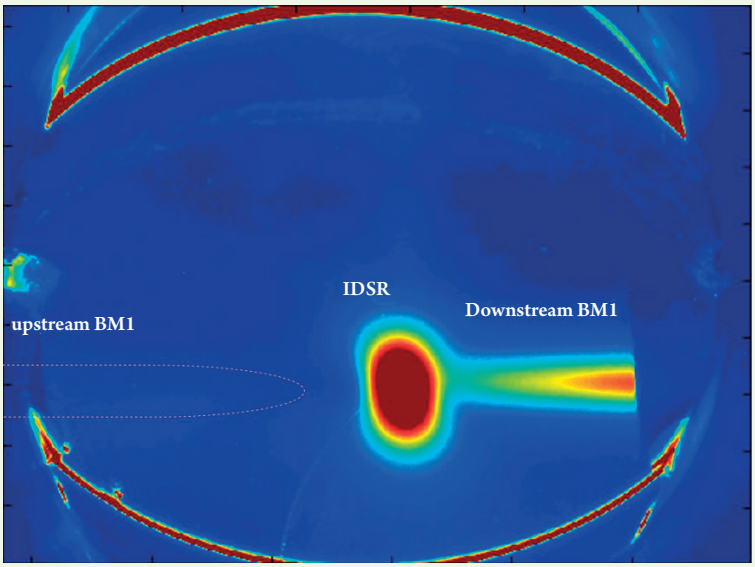

Fig. 3: First IU22 source image obserred at a YAG screen.

raising the temperature, the next 40 h had the temperature in a stable state, and the last 10 h was for decreasing the temperature. During the decreasing temperature, the IP was first switched on for 10 min, then BA gauge/RGA degassing, followed by NEG activation. We achieved the required vacuum criterion (3×10^{-8} Pa) within baking for 70 h. One week after baking, the pressure was $<1.2\times10^{-8}$ Pa. An average pressure of seven IU22 was 9.8×10^{-9} Pa during 30 days after baking. One accident related to water cooling pipe of RF transition taper occurred in the undulator baking, serious vacuum leakage was found. After rigours analysis (Electron probe X-ray Analyzer, SEM and Ion Chromatography), the possible reason may be due to the remaining acid of H_2NO_3 on the copper surface during the clean process. The vacuum excavation will cause the water evaporated and density of H_2NO_3 concentrated. High density of H_2NO_3 becomes erosion on the copper pipe and interacts with copper which produces Cu_2NO_3. High temperature baking turns the Cu_2NO_3 into CuO. Vacuum leakage comes from oxidized surface of cooling pipe.

The accident was quickly repaired on replacing with a new cooling-water pipe and the undulator was baked once more. On July 2, all ten IDs achieved UHV and cooling water was circulating in the ID ready for commissioning.

Commissioning of insertion devices

When a double mini-β Y lattice is optimized using beam-based alignment and the closed-orbit distortion (COD) is minimized, we describe this condition as a *golden orbit*. The first step of in-vacuum undulator commissioning is different from that of an EPU because we must ensure that the upstream bending magnet is not irradiated on the magnet cover. A YAG screen monitor was prepared in the front end to observe the synchrotron radiation spots (two bends and IU). The undulator gap was open at 25 mm to compare the radiation intensity from the bending magnet and the undulator. Three spots should be aligned at the same vertical level to prove that the radiation from the bending magnet can pass through the undulator gap (Fig. 3). The image becomes improved on inserting a copper or alumina filter to stop soft X-rays.

An orbit interlock is essential to protect the mis-steering of an electron beam. This orbit interlock is applicable at the BMP upstream and downstream of the bending magnet that is, in turn, upstream of an undulator (Fig. 4(a)). This precaution is particularly important to protect an IU22 from damage from a mis-steered electron beam in an upstream bending magnet and from its radiation. The criterion for a vertical position interlock is ± 0.1 mm, for the horizontal position interlock ± 1 mm. An orbit interlock for the angle is now under test. The same criterion applies to BMP before and after the EPU and IU22 to avoid image-current heating and ID SR irradiated on the bending vacuum chamber downstream. A double undulator requires more attention because the electron orbit can be kicked by a triplet quadrupole magnets located between ID1 and ID2. The radiation from ID1 might cause a meltdown risk on magnet cover of ID2 (Fig. 4(b)).

Construction of a steering magnet feed-forward table

A pair of horizontal and vertical trim coils is fixed (not movable with a gap) at both ends of every IU22. An auto-measured Matlab script is performed to record the feed-forward table of a trim coil (developed by the beam dynamics group). Upstream and downstream BPMs are used to measure the response matrix using an ID corrector to excite the COD. When the ID gap or phase is altered, we measure a response matrix from the BPMs to calculate the required corrector current to decrease the COD. A two-dimensional feed-forward table is built for an APPLE-II EPU and taper IUT22, and the table allows varied magnetic field operation for all phases, gaps and tapers. Without correction, the RMS orbit distortion (Table 2) due to IU22 about 10–75 μm (H) and 5–15 μm (V). APPLE-II EPU is around 65–140 um (H) and 25–70 um (V). Because the current applied to the steering coil is small, the stability of the power supply becomes important. The IU22 (including the IUT22 taper mode) RMS orbit distortion can be decreased to < 0.5 μm (except IU22-2m vertical RMS COD at beamline I09) for all gaps APPLE-II < 6 um for all gaps and phases, when a feed-forward table is in use. The residual distortion becomes removed with a slow and fast orbit feedback system.

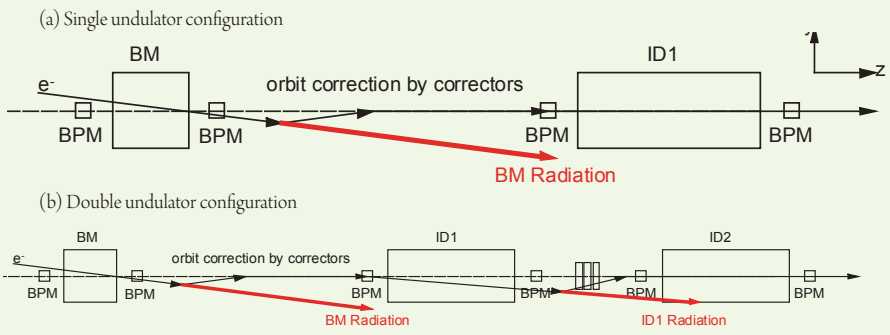

Fig. 4: Schematic of orbit interlock mis-steering.

After we implemented a trim-coil feed-forward table, orbit interlock and orbit feedback system, all IU22 can close the gap to 7 mm. In a double-undulator configuration (cells 5 and 13 in Fig. 5), the pressure in the entire evacuated ring shows that a vertical photon absorber is irradiated with an upstream undulator and a high vacuum pressure is observed. Installation of a vertical photon absorber can prevent an avalanche meltdown caused by heating from upstream ID synchrotron radiation. In December 2015, the maximum

beam current of 250 mA was successful tested with all in-vacuum undulator at minimum gap operation.

Influence of an insertion device on beam parameters

When a feed-forward table of a steering magnet is applied, we close each undulator to test the injection efficiency; there is no obvious change in the IU operation and the APPLE-II EPU horizontal linear mode. We expected that the injection efficiency becomes small when an APPLE-II EPU alters the phase to a vertical linear mode because of a tune shift, which must be corrected with a LOCO algorithm to correct the skew quadrupole components. A tune shift is measured for each ID, shown in Table 2. When seven in-vacuum undulators are near the minimum gap, the vertical tune shift ν_y/ν_x changes are 0.01 and 0, respectively. An in-vacuum undulator center is necessary for fine alignment through creating an orbit vertical bump and measuring the beam lifetime. Table 2 shows that the beam lifetime becomes improved with fine vertical alignment of each IU; this work will be performed in a long shut-down period.

Table 2: RMS COD due to operation of an ID, and effect of IU and EPU on the tuning shift.

Port	ID	Minimum Gap (mm)	Tune shift	RMS COD before correction[1] (μm)	RMS COD after correction[1,2] (μm)
05	IU22	5.6	0/0.003	39 (H) 6 (V)	0.5 (H) 0.1 (V)
09	IU22[(A)]	5.5	0/0.003	75 (H) 6 (V)	0.5 (H) 1.5 (V)
	IU22[(B)]	7	0/0.002	16 (H) 5 (V)	0.3 (H) 0.2 (V)
21	IUT22	5.5	0/0.003	10 (H) 4 (V)	0.4 (H) 0.3 (V)
23	IU22	5.5	0/0.002	41 (H) 15 (V)	0.4 (H) 0.2 (V)
25	IU22[(A)]	5.5	0/0.003	41 (H) 7 (V)	0.5 (H) 0.4 (V)
	IU22[(B)]	7	0/0.002	18 (H) 5 (V)	0.3 (H) 0.2 (V)
41	EPU48[(A)]	13	0.003/0.002	70 (H) 24 (V)	6.0 (H) 1.5 (V)
	EPU48[(B)]	13	0.0075/0.003	137 (H) 29 (V)	4.5 (H) 1.3 (V)
45	EPU46	14	0.0075/0.003	65 (H) 72 (V)	3.0 (H) 1.0 (V)

[1] Beam current operation at I_b=30 mA
[2] Response matrix applied on each gap
[(A)] Upstream undulator
[(B)] Downstream undulator

Challenge of a double-undulator configuration

To maintain the electron beam passing through the sweet spot (effective magnetic field area) of each undulator, two undulators and a quadurople set should be aligned vertically with accuracy ± 50 μm using the same reference position. In double undulator configuration, superimpose of two radiation cones is important to obtain higher flux compare that of a single undulator. As the radia-

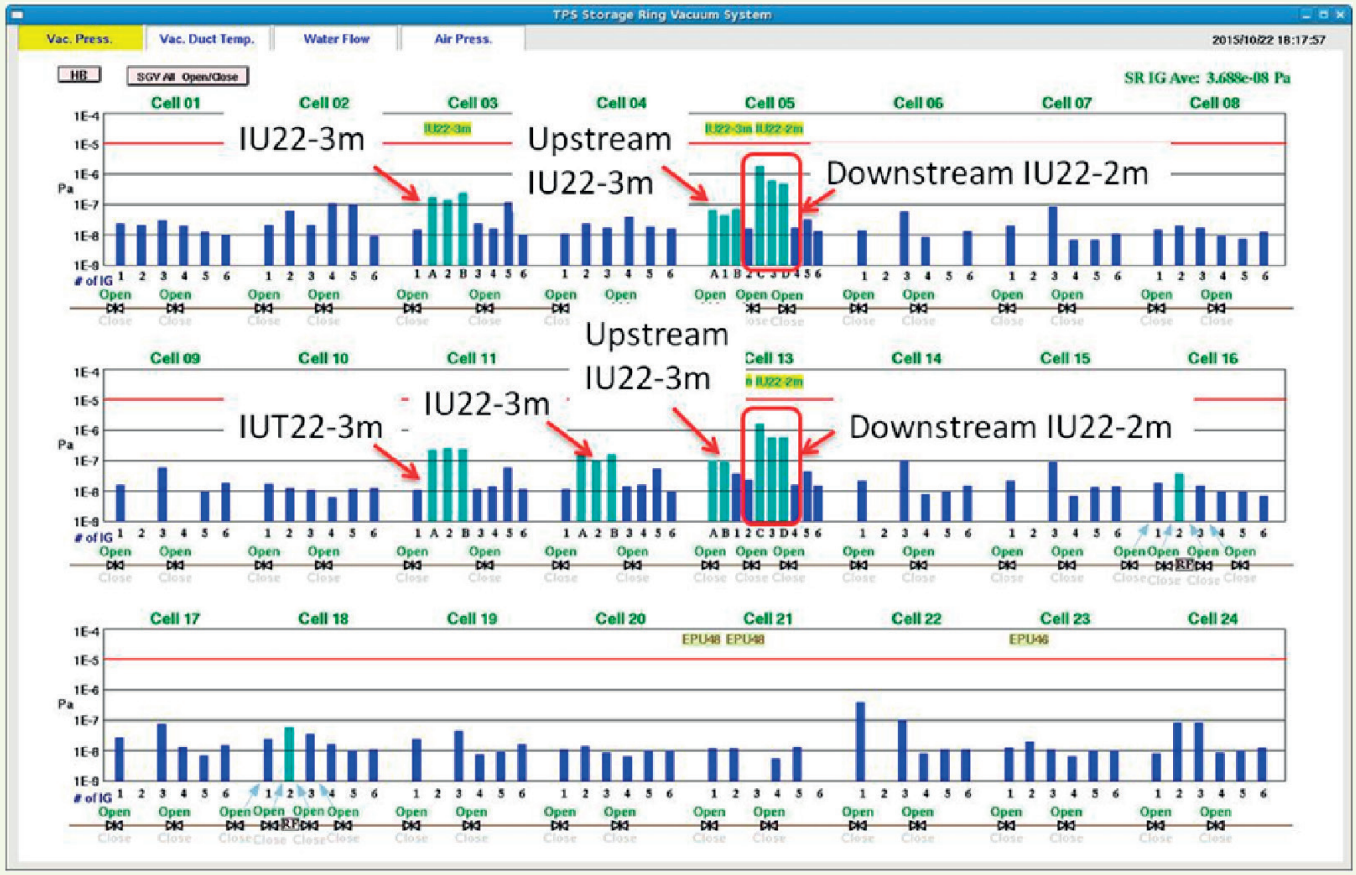

Fig. 5: Vacuum pressure distribution during IU22 commissioning. I_b=30mA.

tion position or direction depends only on the position or direction of the electron beam in undulators, the orbit should be corrected to ensure that the positions and angles of trajectory at ID1 and ID2 are consistent within a tolerance which is 10 % of the electron beam size and divergence. Therefore, at TPS case, the axes of the two wave packets of undulator radiation should fit within ± 1.6/1 μradiana (horizontally and vertically), ± 16/0.5 μm (horizontally and vertically).

Finite kick on the electron orbit can be expected from triplet quadrupole magnet because not all the electrons pass through magnet center and misalignment by triplet qadrupole magnets may cause another kick on electron beam orbit. As a result, two photon beams separate in space can be expected if no orbit correction is applied. For orbit correction between double undulators, two slits/XBPMs are necessary to define the position of the photon beam, maybe one in the front end section and the other in front of the monochromator. The centers of the photon beam can be determined by measuring spectra of photons emitted from individual undulators for different slit transverse positions. Those positions can be converted to the angles and positions of the electron beam injected to individual undulators. These positional errors, thus, can be corrected by two steering magnets installed between segments of IDs.

The drift of a COD or the quadrpole magnetic center due to magnetic aging or ground sink may cause mismatch of two superimposed radiation cones. Orbit correction scheme of double undulator configurations is under development. (Reported by Jui-Che Huang)

Reference

1. J.-C. Huang, H. Kitamura, C.-H. Chang, C.-H. Chang, and C.-S. Hwang, Nucl. Instr. Meth. Phys. Res. **775**, 162 (2015).

Construction and Commissioning of TPS Phase-I Beamlines

Taiwan Photon Source (TPS) is designed to emphasize electron beams of small emittance and great brilliance to generate extremely bright photon beams. These superior characteristics of the TPS have opened avenues of novel scientific opportunities for scientists in several diverse research areas to reveal structures, electron interactions, functions of materials and their dynamics using various spectrometric tools, imaging methods and scattering techniques. At the TPS, seven beamlines in phase I are under construction with advanced techniques including protein microcrystallography (05A), temporally coherent X-ray diffraction (09A), X-ray nanodiffraction (21A), X-ray nanoprobe (23A), coherent X-ray scattering (25A), resonant soft X-ray scattering (41A) and submicron soft X-ray spectroscopy (45A). Listed in Table 1 is a summary of specifications of beamlines in phase I.

After installation of ten undulators and two superconducting RF-cavities in September, the TPS storage ring achieved a stored-electron beam current up to 520 mA, above its design value 500 mA, on Dec. 12, 2015. Beamline optics and experimental end stations of seven beamlines in phase I have been intensively and concurrently installed at the TPS.

While the TPS ramps to its target value of stored current, three beamlines—for protein microcrystallography, for temporally coherent X-ray diffraction and for coherent X-ray scattering—are being commissioned. Up to December 2015, TPS-05 has delivered monochromatic X-rays with beam sizes a few tens of microns and obtained experimental data. X-rays from two collinear IUs installed in the same 12-meter straight section with a double mini-β_y lattice have been monochromatized and transported to the 8-circle diffractometer at beamline TPS-09. At another 12-meter straight section, X-rays from two collinear IUs have been made monochromatic and spectra have been recorded at

Table 1: Summary of specifications of beamlines, phase I.

		05A Protein μ-crystallography	09A Temporally Coherent XRD	21A X-ray Nanodiffraction	23A X-ray Nanoprobe	25A X-ray Coherent Scattering	41A Soft X-ray Scattering	45A Sub-μm Soft X-ray Spectroscopy
Insertion devices		IU22	Tandem IU22	Tapered IU22	IU22	Tandem IU22	Tandem EPU48	EPU46
Energy range		5.7–20 keV	5.6–25 keV	7–25 keV	4–15 keV	5.5–20 keV	400–1200 eV	280–1500 eV
Experimental techniques								
Imaging (CDI)					•	•	•	
Scattering	Structural diffraction	•	•	•	•	•	•	
	Scattering					•	•	
Spectroscopy	XAS		•	•	•	•	•	•
	XEOL			•	•			•
	RIXS						•	•
	PES							•

CDI: coherent diffraction imaging
XAS: X-ray absorption spectroscopy
XEOL: X-ray excited optical luminescence
RIXS: resonant inelastic X-ray scattering
PES: photoemission emission spectroscopy